International Journal of Chemical and Biochemical Sciences
(ISSN 2226-9614)

Journal Home page: www.iscientific.org/Journal.html

Bis(4-dimethylaminodithiobenzil)M, (M=Ni, Pd, or Pt) electronic, thermodynamic and spectroscopic properties as a laser dye: A DFT study

Mudar A Abdulsattar[1*], A A Jabor[1], Z T Hussain[1], A H Khalid[1], S A Alkharkhe[2]

[1]*Ministry of Science and Technology, Baghdad, Iraq.*

[2]*Department of Biology, College of Education for Pure Science, University of Diyala, Diyala, Iraq.*

Abstract

Density functional theory is used to calculate electronic, thermodynamic, and spectroscopic properties of bis(4-dimethylaminodithiobenzil)M, (M=Ni, Pd, or Pt). These complexes can also be written as $C_{32}H_{30}N_2S_4M$ (M=Ni, Pd, or Pt). Calculated properties include energy gaps, UV-Vis spectra, bond lengths, atomic charges, vibrational reduced masses, vibrational force constants, Raman spectra, Gibbs free energy, enthalpy, the entropy of atomization, and heat capacity. Our results show that the energy gap of the Pd complex at 1016 nm is the closest to the Nd:YAG laser energy at 1064 nm. Electron affinity of the metallic elements Ni, Pd, and Pt can interpret many properties. Pt, Ni, and Pd have the highest electron affinity in order, respectively. This order is also followed by charges, energy gaps, vibrational frequency gaps, Gibbs free energy, enthalpy, and entropy of atomization. Other quantities such as heat capacity do not follow this order indicating other factors affecting such quantities. One of the distinctive features of these complexes is the Raman M-S breathing mode at 357, 364 and 383 cm^{-1} for Ni, Pd, and Pt respectively that can be used in identification of these complexes.

Keywords: Laser dye, Density functional theory, Gibbs free energy, Raman spectra

Full length article **Corresponding Author,* e-mail: mudarahmed3@yahoo.com

1. Introduction

Bis(4-dimethylaminodithiobenzil)M, (M=Ni, Pd, or Pt) is used as a dye for laser Q-switched saturable absorber [1,2,11–18,3–10]. The chemical formula of these complexes is $C_{32}H_{30}N_2S_4M$ (M=Ni, Pd, or Pt). In these complexes, the central atom (Ni, Pd, or Pt) is attached to four sulfur atoms (S) as in figure 1. Each one of the S atoms is connected to a carbon atom that is attached to a phenyl group (C_7H_5) or to a carbon atom that is linked to phenyl group with dimethylamine group ($C_7H_4N(CH_3)_2$). The usual central atom is Ni. However, Ni being in group 10 of elements, it can be interchangeable with both Pd and Pt [19,20,29,30,21–28]. The three compounds can be abbreviated as BDNi, BDPd, and BDPt for Ni, Pd, and Pt complexes respectively. Experimental bond lengths between Ni, Pd, or Pt atoms with S atoms and other useful data can be found in other compounds in literature [31–35]. All calculations will be performed using the Gaussian 09 program [36,37].

This work aims to analyze the electronic thermodynamic, and spectroscopic structure of bis(4-dimethylaminodithiobenzil)M, (M=Ni, Pd, and Pt). This includes energy gapes, UV-Vis, bond lengths, vibrational reduced masses, force constants, and atomic charges. Thermodynamic quantities such as Gibb free energy, enthalpy, and entropy of atomization in addition to heat capacity is to be evaluated. Density functional theory (DFT) can be used to produce accurately all the quantities mentioned above and even quantities that are difficult to be evaluated experimentally such as orbital electron occupation as we shall see in results section.

2. Methods/Theory

Bis(4-dimethylaminodithiobenzil)Ni is shown in figure 1. As we can see from this figure that two of the arms that branch from the four S atoms connected to Ni atoms (C_7H_5) are shorter than the other two arms ($C_7H_4N(CH_3)_2$). The shorter arms are abbreviated (Sh arms) while the longer arms are abbreviated (L arms). As we shall see later that the kind of arm that is connected to an S atom (figure 1) affects the charge, bond length, force constant, and reduced mass of vibration. Density functional theory (DFT) at the B3LYP level will be used to analyze the present molecules. 6-311G** basis functions will be used to represent the atomic orbitals of C, N, S, and H. These functions cannot be used for the heavier atoms Pd and Pt. The SDD basis states

(Stuttgart/Dresden) effective core potentials are available for all the three elements Ni, Pd, and Pt [37]. Vibrational scale factors are used to correct frequencies so that theoretically calculated vibrations are near experimental results. Scale factors associated with B3LYP/6-311G** and B3LYP/SDD are 0.967 and 0.961, respectively [37]. All the atom's orbitals (68 atoms) are managed using B3LYP/6-311G** theory except one atom (the metallic atom) in each complex. An average scale factor of 0.967 is used in the present calculations.

3. Results and Discussions

Fig 2 shows the calculated UV-Vis spectra of the Ni, Pd, and Pt. Our results are in good agreement with the experimental results of reference [3] for BDNi. The value of the wavelength of the Nd:YAG laser at 1064 nm (1.165 eV at the infrared region) is shown in figure 2. It can be seen that BDPd spectrum peak is the closest to the Nd:YAG laser at 1064 nm as predicted by present calculations. At 200-400 nm, a peak that corresponds to the phenyl group can be seen. The three peaks 952, 1016, 944 nm corresponds to the maximum peaks of Ni, Pd and Pt UV-Vis spectrum respectively.

Figure 3 shows the reduced masses of Raman vibrations of BDNi as calculated by present theory. The masses of H and C are shown to distinguish between vibrations of different atoms. The frequency gap boundaries are also shown. The vibrations with reduced mass near 1 are vibrations due to hydrogen. According to the frequency proportionality rule:

$$\nu \sim \sqrt{\frac{k}{m}}, \qquad (1)$$

the frequency (ν) is proportional to the force constant (k) and inversely proportional to the mass (m). As a result, we expect that Ni vibrations are in the beginning and H vibrations are at the end. This is true as we can see in figure 3. The highest reduced masses are at ν=357.181 cm-1, which is called the Ni-S breathing mode [38]. H-C vibrations are the last vibrations around 3000 cm-1. Since the H mass is very smaller than other atoms, a frequency gap is between H vibrations and the other vibrations. This gap starts at 1593.704 cm-1 for C-C vibrations and ends at 2879.428 cm-1 for BDNi. Figure 4 shows vibrational force constants of the different bonds in BDNi. The strongest bonds are C-C bonds at the beginning of the frequency gap. H vibrations also have high force constants while the smallest force constants are for the heavy atoms at the beginning of the spectrum. Figure 5 shows the Raman intensity spectrum of BDNi. All the vibrations mentioned previously exist in this spectrum. However, the peak that distinguishes this spectrum from many other materials is the Ni-S breathing mode at 357.181 cm-1. The breathing mode is characterized by the movement of S atoms simultaneously towards or away from the Ni atom as in figure 6. Natural bond orbital (NBO) analysis is performed to find the kind of charges that exist on each atom in the three complexes as in figure 7. The kind of charges at the central atoms is shown in figure 7, while Table 1 summarizes all other charges that include NBO analysis of the three complexes. Table 1 also shows thermodynamic quantities that include Gibbs free energy, enthalpy, the entropy of atomization and heat capacity. These thermodynamic quantities are evaluated at Standard Ambient Temperature and Pressure (SATP) that are 298.150 Kelvin and a pressure of 1 atmosphere.

The electronic affinities (EA) of the three elements Ni, Pd, and Pt are 1.156, 0.562, and 2.128 eV, respectively [35]. Pt has the highest EA, followed by Ni and Pd. The electronic charges on the three elements Ni, Pd, and Pt follow the order imposed by the EA so that the highest charge is at Pt followed by Ni and finally Pd. The most affected charges by this order are electronic charges on S atoms from which charges are absorbed according to the electron affinity of the central metal. This effect on charges decreases as we go far from the central metallic ions. As an example, N and H are the least affected atoms by the electron affinity of the metals as we can see in Table 1. The effect of EA is not limited to charges; it can be extended to energy gap, vibrational and thermodynamic properties. The highest energy gap in Table (1) is for Pt followed by Ni ad finally Pd. This order can be interpreted by EA by noting that the element with high EA absorbs charges from the levels inside the energy gap and as a result widens the energy gap. The reverse effect can be found in the frequency energy gap. The three thermodynamic quantities Gibbs free energy, enthalpy, and entropy follow the order of EA. However, other quantities such as the heat capacity don't follow the order of EA that indicate other factors affecting such quantities. Finally, the electron configuration of the three elements Ni, Pd, and Pt is shown in Table (1). Orbitals with less than 0.01 electrons are not shown in the Gaussian 09 program used for present calculations. The number of orbitals with charges greater than 0.01 electron decreases as the element charge increases. This indicates that elements with smaller charges have their electronic charges distributed on higher orbitals as in Table 1.

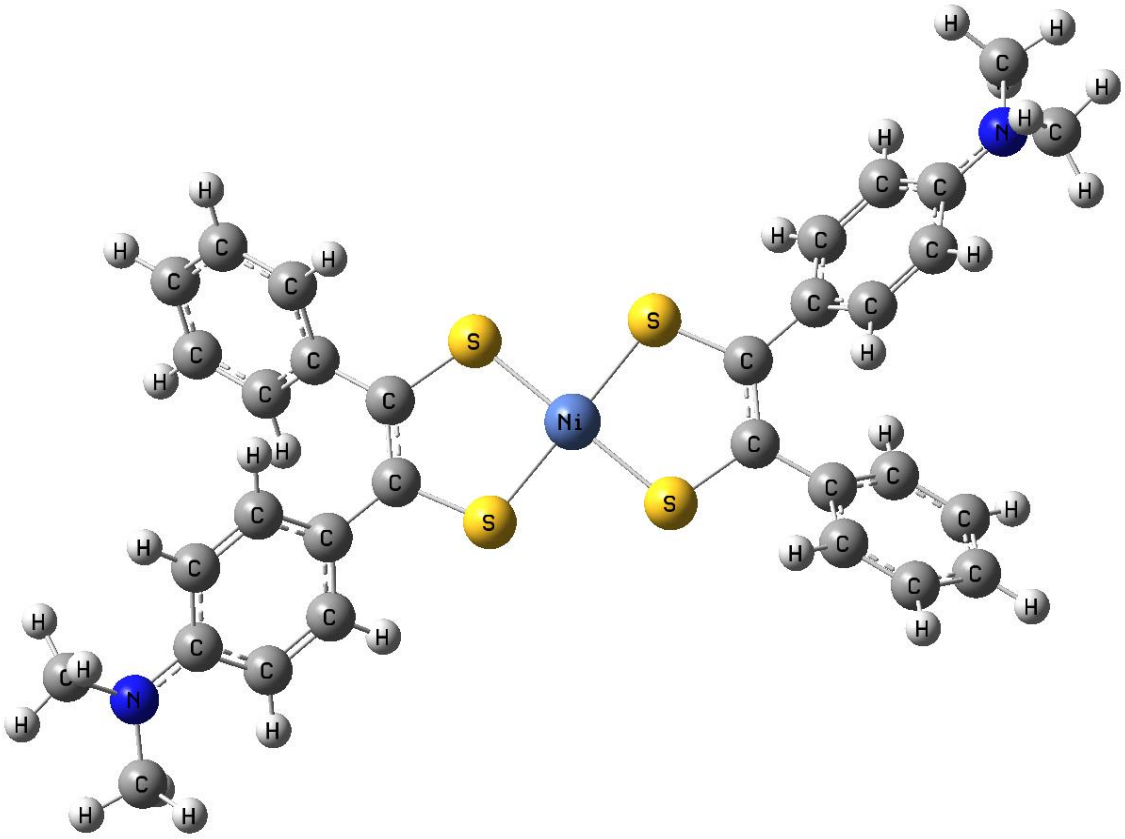

Figure 1: bis(4-dimethylaminodithiobenzil)Ni after geometrical optimization.

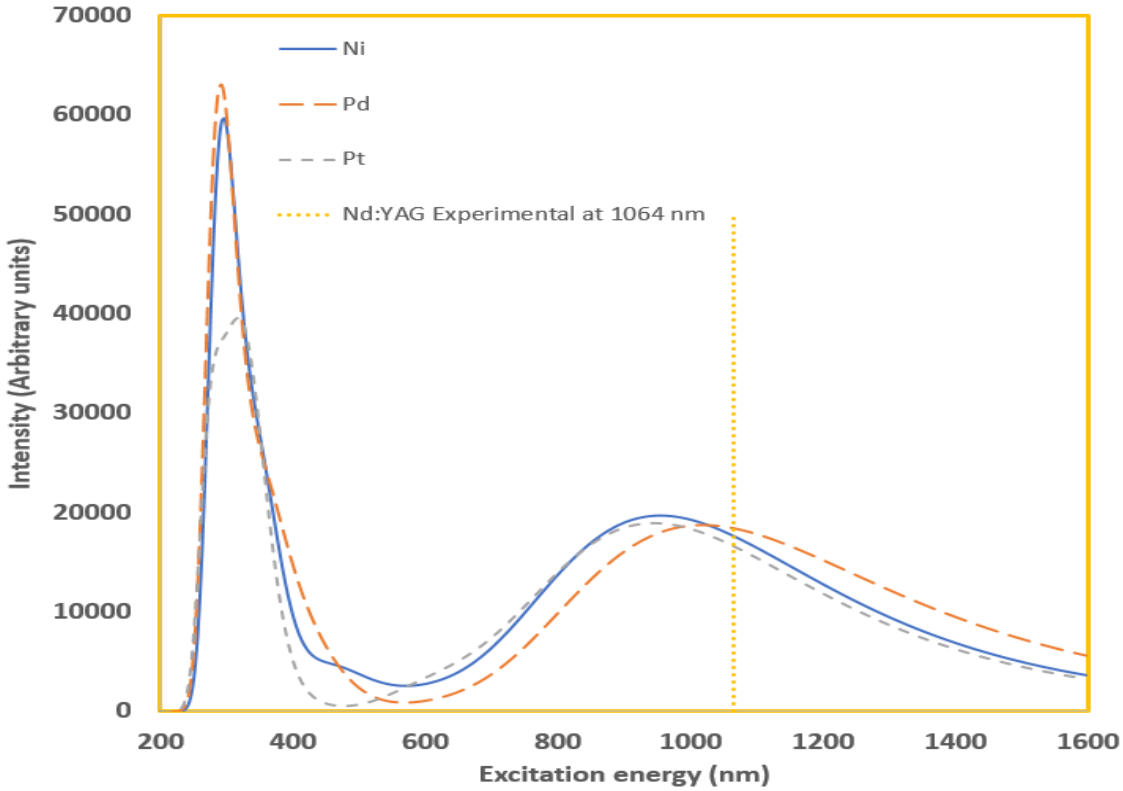

Figure 2: Calculated UV-Vis of the three complexes BDNi, BDPd, and BDPt. The experimental Nd:YAG laser at 1064 nm is also shown.

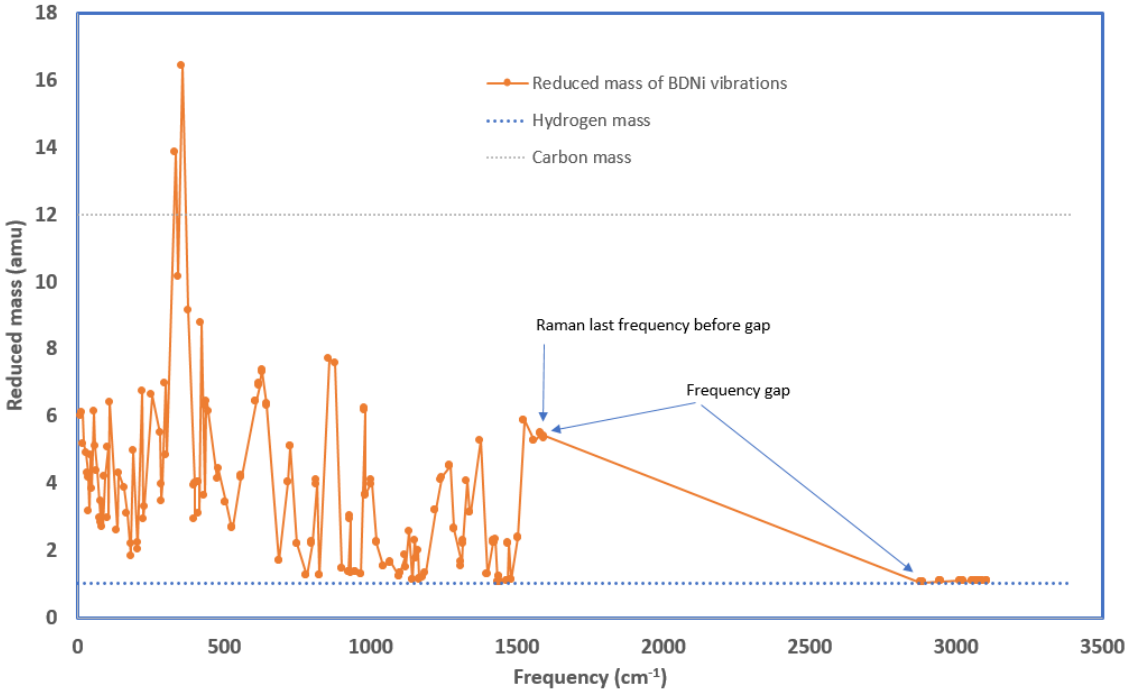

Figure 3: Reduced masses of BDNi Raman vibrations. The masses of H and C are shown. The frequency gap boundaries are also shown.

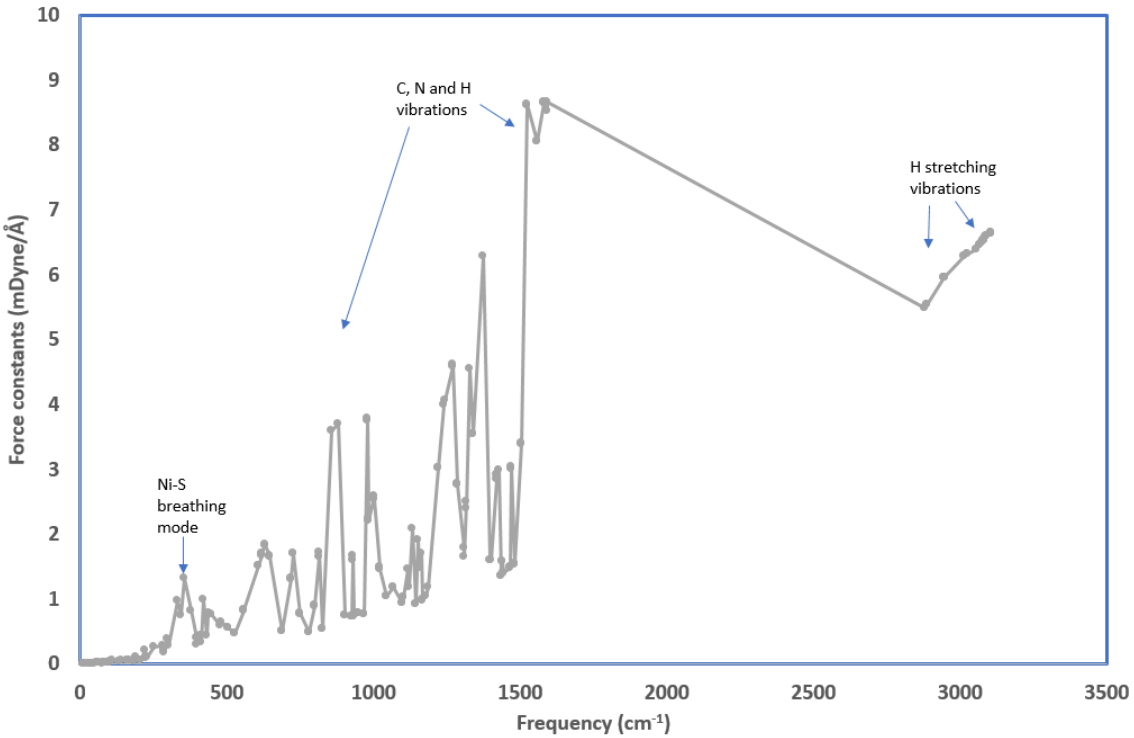

Figure 4: Force constants of BDNi Raman vibrations.

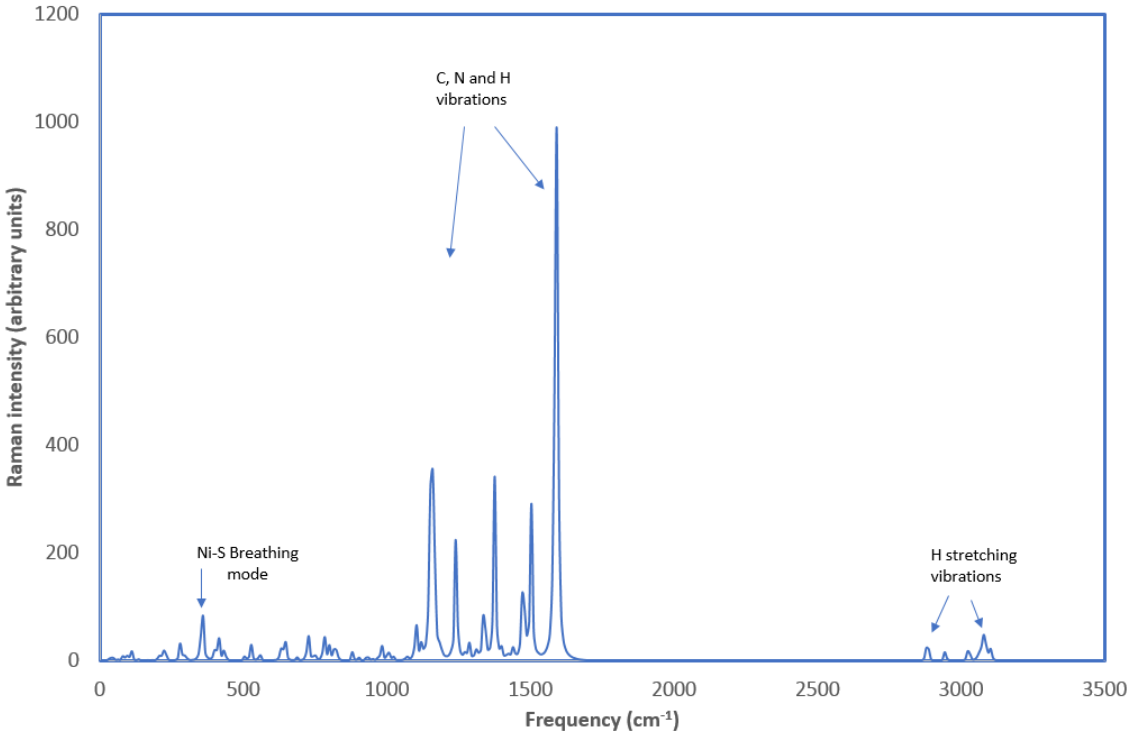

Figure 5: Raman spectrum of BDNi vibrations.

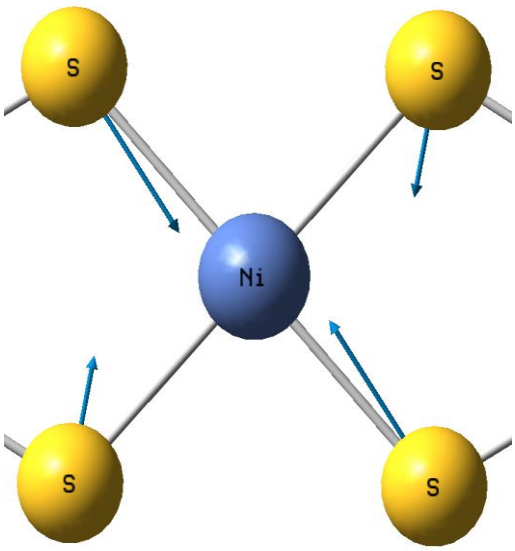

Figure 6: Ni-S Raman breathing mode of BDNi at 357.181 cm^{-1}. Displacement vectors are shown.

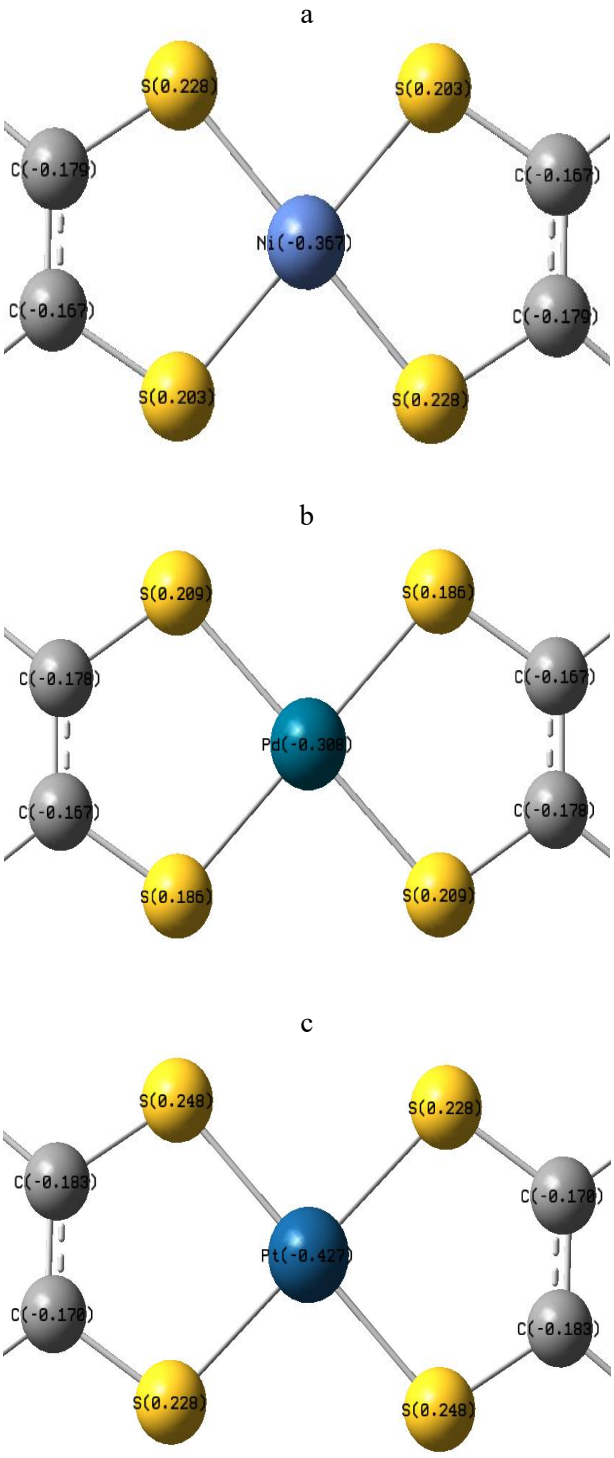

Figure 7: (a) BDNi charges, (b) BDPd charges and (c) BDPt charges.

Table 1: Comparison of different properties of the three complexes BDNi, BDPd, and BDPt. Abbreviations used in the table are: M=metal (either Ni, Pd or Pt), L=Long arm, Sh=Short arm, a.u.=atomic units.

Property	BDNi	BDPd	BDPt
Bond length M-S(L) (Å)	2.1729	2.307	2.313
Bond length M-S(Sh) (Å)	2.1666	2.301	2.305
HOMO-LUMO energy gap (eV)	1.386	1.183	1.407
Raman M-S breathing mode (cm^{-1})	357.181	363.708	382.516
Raman last frequency before gap (cm^{-1})	1593.704	1593.348	1594.626
Raman frequency gap (cm^{-1})	1285.724	1286.879	1283.722
Charge on M (a.u.)	-0.357	-0.308	-0.427
Charge on S(L) (a.u.)	0.203	0.186	0.228
Charge on S(Sh) (a.u.)	0.228	0.209	0.248
Charge on C(L) (a.u.)	-0.167	-0.167	-0.170
Charge on C(Sh) (a.u.)	-0.179	-0.178	-0.183
Charge on N (a.u.)	-0.435	-0.434	-0.436
Charge on H (a.u.)	0.18-0.214	0.18-0.214	0.18-0.213
Gibbs energy of atomization (eV)	-292.632	-292.294	-294.022
Enthalpy of atomization (eV)	-318.286	-317.908	-319.686
Entropy of atomization (Cal/Mol-K)	-1984.166	-1981.065	-1984.71
Heat capacity (Cal/Mol-K)	144.141	144.563	144.492
Natural electron configuration of M	[core]$4s^{0.46}$ $3d^{8.94}$ $4p^{0.94}$ $4d^{0.01}$	[core]$5s^{0.48}$ $4d^{9.12}$ $5p^{0.69}$ $5d^{0.01}$ $6d^{0.01}$ $7p^{0.01}$	[core]$6s^{0.66}$ $5d^{8.98}$ $6p^{0.77}$

4. Conclusions

The electronic, vibrational, and thermodynamic properties of the three complexes BDNi, BDPd, and BDPt are calculated. Bonds that connect the central metallic atom to surrounding S toms are affected by the structure of the molecule. Raman M-S vibrational breathing mode increases with the mass of the metal. Results show that the Pd complex is more appropriate and closer than the other two elements (Ni ant Pt) to the Nd:YAG laser energy at 1064 nm. Electron affinity of the central metallic elements showed the ability to interpret many of the calculated properties. Pt, Ni, and Pd have the highest electron affinity, respectively. This order is also noticed in charges, energy gaps, vibrational frequency gaps, Gibbs free energy, enthalpy and entropy of atomization. Other quantities such as heat capacity do not follow the order imposed by electron affinity showing that they are affected by other factors.

References

[1] T. Moncond'Huy, L. Bastard, F. Royer, M.-F. Blanc-Mignon, Development of sol-gel saturable absorber for integrated Q-switched lasers, in: Proceedings of SPIE - The International Society for Optical Engineering, 2017. https://doi.org/10.1117/12.2251443.

[2] H. Ouslimani, L. Bastard, J.-E. Broquin, Narrow-linewidth Q-switched DBR laser on Ytterbium-doped glass, Ceramics International. 41 (2015) 8650–8654. https://doi.org/10.1016/j.ceramint.2015.03.076.

[3] S. Dalgleish, M.M. Matsushita, L. Hu, B. Li, H. Yoshikawa, K. Awaga, Utilizing photocurrent transients for dithiolene-based photodetection: Stepwise improvements at communications relevant wavelengths, Journal of the American Chemical Society. 134 (2012) 12742–12750. https://doi.org/10.1021/ja304228c.

[4] B. Charlet, L. Bastard, J.-E. Broquin, Integrated optics dissipative soliton mode-locked laser on glass, in: Proceedings of SPIE - The International Society for Optical Engineering, 2011. https://doi.org/10.1117/12.873782.

[5] R. Salas-Montiel, L. Bastard, G. Grosa, J.-E. Broquin, Hybrid Neodymium-doped passively Q-switched waveguide laser, Materials Science and Engineering B: Solid-State Materials for Advanced Technology. 149 (2008) 181–184. https://doi.org/10.1016/j.mseb.2007.11.012.

[6] Y. Wan, D.-Y. Zhu, Q.-Y. Zeng, Z.-Y. Zhang, J. Zhang, K. Han, Brewster-oriented passive Q-switch intracavity optical parametric oscillator, Chinese Physics. 14 (2005) 714–719. https://doi.org/10.1088/1009-1963/14/4/013.

[7] H. Li, K. Ogusu, Optical nonlinearities of Bis(4-dimethylaminodithiobenzil)-nickel solution in the nanosecond regime, Japanese Journal of Applied Physics, Part 1: Regular Papers and Short Notes and Review Papers. 37 (1998) 5572–5577. https://doi.org/10.1143/jjap.37.5572.

[8] Y. Yokota, K. Ogusu, Y. Tanaka, Focused-beam-induced diffraction rings from an absorbing solution, IEICE Transactions on Electronics. E81-C (1998) 455–460.

[9] K. Ogusu, Y. Kohtani, H. Shao, Laser-induced diffraction rings from an absorbing solution, Optical Review. 3 (1996) 232–234. https://doi.org/10.1007/s10043-996-0232-1.

[10] M. Szczurek, Mode-locked Nd:YAG laser with intracavity phase conjugate mirror, Optics Communications. 61 (1987) 42–44. https://doi.org/10.1016/0030-4018(87)90121-0.

[11] R.C. Greenhow, D.M. Goodall, R.W. Eason, Ground-state repopulation time of BDN I and BDN II in a variety of solvent and plastic hosts, Chemical Physics. 83 (1984) 445–450. https://doi.org/10.1016/0301-0104(84)85018-1.

[12] D. Lala, J.F. Rabek, Photo-stabilising effect of Ni compounds in photo-oxidative degradation of cis-1,4-poly(butadiene), Polymer Degradation and Stability. 3 (1981) 383–396. https://doi.org/10.1016/0141-3910(81)90044-6.

[13] R.C. Greenhow, A.J. Street, Mode Locking the Nd : Glass Laser with BDN: Measurements of Dye Recovery Times and Laser Pulse Lengths, IEEE Journal of Quantum Electronics. 11 (1975) 59–60. https://doi.org/10.1109/JQE.1975.1068516.

[14] D. Magde, B.A. Bushaw, M.W. Windsor, Picosecond flash photolysis and spectroscopy: Bis-(4-dimethylaminodithiobenzil)-Ni(II), BDN, Chemical Physics Letters. 28 (1974) 263–269. https://doi.org/10.1016/0009-2614(74)80069-2.

[15] D. Magde, B.A. Bushaw, M.W. Windsor, Q Switching and Mode Locking the Nd3+–Glass Laser with the Nickel Dithienes, IEEE Journal of Quantum Electronics. 10 (1974) 394–395. https://doi.org/10.1109/JQE.1974.1068148.

[16] D. Magde, B.A. Bushaw, M.W. Windsor, Q SWITCHING AND MODE LOCKING THE Nd^{3+}-GLASS LASER WITH THE NICKEL DITHIENES., IEEE Journal of Quantum Electronics. QE-10 (1974).

[17] K.H. Drexhage, U.T. Mueller-Westerhoff, NEW Q-SWITCH COMPOUNDS FOR INFRARED LASERS., IEEE Journal of Quantum Electronics. QE-9 (1972).

[18] K.H. Drexhage, U.T. Müller-Westerhoff, New Q-Switch Compounds for Inrared Lasers, IEEE Journal of Quantum Electronics. 8 (1972) 759. https://doi.org/10.1109/JQE.1972.1077284.

[19] V.M. Rendón-López, Á.J.A. Castro, J.C. Alvarado Monzón, C. Cristóbal, G.G. Gonzalez, S.G. Montiel, O. Serrano, J.A. Lopez, Ni(II), Pd(II) and Pt(II) complexes with SacNac tridentate ligand, Polyhedron. 162 (2019) 207–218. https://doi.org/10.1016/j.poly.2019.01.021.

[20] R.G. Mohamed, F.M. Elantabli, A.A. Abdel Aziz, H. Moustafa, S.M. El-Medani, Synthesis, characterization, NLO properties, antimicrobial, CT-DNA binding and DFT modeling of Ni(II), Pd(II), Pt(II), Mo(IV) and Ru(I) complexes with NOS Schiff base, Journal of Molecular Structure. 1176 (2019) 501–514. https://doi.org/10.1016/j.molstruc.2018.08.113.

[21] K.J. Al-Adilee, H.K. Dakheel, Synthesis, spectral and biological studies of Ni(II), Pd(II), and Pt(IV) complexes with new heterocyclic ligand derived from Azo-schiff bases dye, Eurasian Journal of Analytical Chemistry. 13 (2018). https://doi.org/10.29333/ejac/97267.

[22] P. Romaniello, F. Lelj, Limits in the second-order response of [M(H<inf>2</inf>imXdt) (H <inf>2</inf>imYdt)] neutral complexes (M = Ni, Pd, Pt; H<inf>2</inf>imXdt = monoanion of imidazolidine-2-chalcogenone-4,5-dithione; X = O, S, Se; Y = O, S, Se; X ≠ Y): A pure theoretical stu,

Journal of Molecular Structure: THEOCHEM. 636 (2003) 23–37. https://doi.org/10.1016/S0166-1280(03)00349-X.

[23] M.A. Arafath, F. Adam, M.R. Razali, L.E. Ahmed Hassan, M.B.K. Ahamed, A.M.S.A. Majid, Synthesis, characterization and anticancer studies of Ni(II), Pd(II) and Pt(II) complexes with Schiff base derived from N-methylhydrazinecarbothioamide and 2-hydroxy-5-methoxy-3-nitrobenzaldehyde, Journal of Molecular Structure. 1130 (2017) 791–798. https://doi.org/10.1016/j.molstruc.2016.10.099.

[24] S. Rabaça, S. Oliveira, D. Belo, I.C. Santos, M. Almeida, Complexes with pyrazine-tetrathiafulvalene-dithiolate (pztdt) ligand [M(pztdt)<inf>2</inf>], M = Ni, Pd, Pt; Synthesis and characterisation, Inorganic Chemistry Communications. 58 (2015) 87–90. https://doi.org/10.1016/j.inoche.2015.06.001.

[25] M. Gaber, H.A. El-Ghamry, S.K. Fathalla, Ni(II), Pd(II) and Pt(II) complexes of (1H-1,2,4-triazole-3-ylimino)methyl]naphthalene-2-ol. Structural, spectroscopic, biological, cytotoxicity, antioxidant and DNA binding, Spectrochimica Acta - Part A: Molecular and Biomolecular Spectroscopy. 139 (2015) 396–404. https://doi.org/10.1016/j.saa.2014.12.057.

[26] A.A.S. Al-Hamdani, A.M. Balkhi, A. Falah, S.A. Shaker, New Azo-Schiff base derived with Ni(II), Co(II), Cu(II), Pd(II) and Pt(II) Complexes: Preparation, spectroscopic investigation, structural studies and biological activity, Journal of the Chilean Chemical Society. 60 (2015) 2774–2785. https://doi.org/10.4067/S0717-97072015000100003.

[27] M. Gaber, H. El-Ghamry, F. Atlam, S. Fathalla, Synthesis, spectral and theoretical studies of Ni(II), Pd(II) and Pt(II) complexes of 5-mercapto-1,2,4-triazole-3-imine-2′-hydroxynaphyhaline, Spectrochimica Acta - Part A: Molecular and Biomolecular Spectroscopy. 137 (2015) 919–929. https://doi.org/10.1016/j.saa.2014.09.015.

[28] I.P. Ferreira, G.M. De Lima, E.B. Paniago, J.A. Takahashi, C.B. Pinheiro, Synthesis, characterization and antifungal activity of new dithiocarbamate-based complexes of Ni(II), Pd(II) and Pt(II), Inorganica Chimica Acta. 423 (2014) 443–449. https://doi.org/10.1016/j.ica.2014.09.002.

[29] S. Alyar, N. Özbek, S.Ö. Yildirim, S. Ide, R.J. Butcher, Experimental and computational study on 2,2′-[(1E,2E)-hydrazine-1,2- diylidenedi(1E)eth-1-yl-1-ylidene]diphenol and its Ni(II), Pt(II), Pd(II) complexes, Spectrochimica Acta - Part A: Molecular and Biomolecular Spectroscopy. 130 (2014) 198–207. https://doi.org/10.1016/j.saa.2014.03.034.

[30] K. Zhou, S. Min, G. Xue, W. Huang, Theoretical study of the structure, bonding and electronic behaviour of sandwich complexes [M3(C7H7)2X3]− (M = Ni, Pd, Pt; X = F, Cl), Chemical Physics Letters. 610–611 (2014) 234–240. https://doi.org/10.1016/j.cplett.2014.07.028.

[31] J.E. Demuth, D.W. Jepsen, P.M. Marcus, Small Ni-S bond lengths in a c(2 × 2) overlayer of sulfur on Ni (001), Solid State Communications. 13 (1973) 1311–1313. https://doi.org/10.1016/0038-1098(73)90156-7.

[32] J. Wang, Q. Wang, X. Jiang, Z. Liu, W. Yang, A.I. Frenkel, Determination of nanoparticle size by measuring the metal-metal bond length: The case of palladium hydride, Journal of Physical Chemistry C. 119 (2015) 854–861. https://doi.org/10.1021/jp510730a.

[33] A.G. Daniel, N.P. Farrell, The dynamics of zinc sites in proteins: Electronic basis for coordination sphere expansion at structural sites, Metallomics. 6 (2014) 2230–2241. https://doi.org/10.1039/c4mt00213j.

[34] X. Lin, N.J. Ramer, A.M. Rappe, K.C. Hass, W.F. Schneider, B.L. Trout, Effect of particle size on the adsorption of O and S atoms on Pt: A density-functional theory study, Journal of Physical Chemistry B. 105 (2001) 7739–7747. https://doi.org/10.1021/jp011133p.

[35] N.A. Lange, Lange's Handbook of Chemistry, 15th ed., McGraw-Hill, New York, 1999.

[36] M.J. Frisch, G.W. Trucks, H.B. Schlegel, G.E. Scuseria, M.A. Robb, J.R. Cheeseman, G. Scalmani, V. Barone, B. Mennucci, G.A. Petersson, H. Nakatsuji, M. Caricato, X. Li, H.P. Hratchian, A.F. Izmaylov, J. Bloino, G. Zheng, J.L. Sonnenberg, M. Hada, M. Ehara, K. Toyota, R. Fukuda, J. Hasegawa, M. Ishida, T. Nakajima, Y. Honda, O. Kitao, H. Nakai, T. Vreven, J.A.J. Montgomery, J.E. Peralta, F. Ogliaro, M. Bearpark, J.J. Heyd, E. Brothers, K.N. Kudin, V.N. Staroverov, R. Kobayashi, J. Normand, K. Raghavachari, A. Rendell, J.C. Burant, S.S. Iyengar, J. Tomasi, M.

Cossi, N. Rega, J.M. Millam, M. Klene, J.E. Knox, J.B. Cross, V. Bakken, C. Adamo, J. Jaramillo, R. Gomperts, R.E. Stratmann, O. Yazyev, A.J. Austin, R. Cammi, C. Pomelli, J.W. Ochterski, R.L. Martin, K. Morokuma, V.G. Zakrzewski, G.A. Voth, P. Salvador, J.J. Dannenberg, S. Dapprich, A.D. Daniels, Ö. Farkas, J.B. Foresman, J. V. Ortiz, J. Cioslowski, D.J. Fox, Gaussian 09, Revision D.01, (2013).

[37] R.D. Johnson, NIST Computation Chemistry Comparison and Benchmark Database, NIST Standard Reference Database Number 101 Release 14, (2006). https://doi.org/10.18434/T47C7Z.

[38] C. Kittel, Introduction to solid state physics, New York, 2005. https://doi.org/10.1007/978-3-540-93804-0.